Applied Thermal Engineering 279 (2025) 127862

Contents lists available at ScienceDirect

Applied Thermal Engineering

journal homepage: www.elsevier.com/locate/apthermeng

Research Paper

Kinetic study on the effect of circulating ash on the SNCR deNO$_x$ process based on an improved micro fluidized bed experimental method

Ling Jiang [a], Xueyu Tang [a,b], Dan Li [b,c], Bingjun Du [a,b], Xin Yu [b], Zhong Huang [a,b,c], Xiwei Ke [b,c,*], Junfu Lyu [a,b,c,**]

[a] Department of Energy and Power Engineering, Tsinghua University, Beijing 100084, China
[b] Shanxi Research Institute of Huairou Laboratory, Taiyuan 030032, China
[c] Beijing Huairou Laboratory, Beijing 101499, China

ARTICLE INFO

Keywords:
Circulating ash
NO_x emission
SNCR
CFB boiler
Micro fluidized bed reactor

ABSTRACT

A large number of reactive bed materials in the circulating fluidized bed (CFB) boiler has significant effects on the selective non-catalytic reduction (SNCR) performance and NO_x emission, especially under low-load conditions. In this study, a micro fluidized bed reactor was used to quantitatively analyze the catalytic effect of circulating ash on the NH_3+NO(+O_2) reactions. Results show that the gas–solid fluidization state significantly affects the gas mass transfer resistance in the micro fluidized bed. To minimize the interference of mass transfer resistance on the determination of intrinsic kinetic parameters, for Geldart A particles, it is necessary to precisely adjust the operating parameters to control the fluidization state within the particulate fluidization region. Based on the improved micro fluidized bed experimental method, it was found that under anoxic conditions, coal ash can evidently improve the reduction of NO by NH_3. Under aerobic conditions, it may simultaneously catalyze two rival reactions: SNCR reaction (NO reduction) and NH_3 oxidation (NO formation). For Weihe anthracite coal (WH) ash and Indonesian lignite coal (IN) ash, net reduction on NO is only exhibited under low-oxygen and relatively high-NO-concentration conditions, and the effect of IN ash on NO reduction is more obvious at higher temperatures. However, for Shuozhou bituminous coal (SZ) ash, net NO generation occurs under most operating conditions, indicating that this ash has a negative effect on SNCR denitrification. This study provides guidance for formulating differentiated SNCR denitrification strategies for CFB boilers based on the characteristics of bed materials.

1. Introduction

To construct a new power system with new energy as the main body and accommodate a large proportion of renewable energy power such as wind power and photovoltaic power, which are volatile, intermittent, and random, most coal-fired circulating fluidized bed (CFB) boiler units need to undertake deep peak regulation task and operate at low loads for a long time [1]. As the load decreases, the boiler operating parameters as well as operating performance, including gas–solid fluidization state and bed temperature, may change significantly. For example, CFB boiler usually operates with fast fluidization state under high load conditions. While, when the load drops, the flue gas velocity decreases remarkably, and the overall fluidization state is more like that of a bubbling bed [2].

Change in the fluidization state will alter heat and mass transfer characteristics, thereby affecting gas and temperature distributions in the furnace and indirectly influencing the conversion behavior of nitrogen oxides [3]. More importantly, under low-load conditions, to ensure the safe fluidization of bed materials, high excess air coefficient and high primary air volume are usually adopted, which enhances the oxidizing atmosphere in the furnace and promotes the NO_x generation. Studies have shown that when the load ratio of a CFB boiler is lower than 50 %, as the load further decreases, the NO_x emission increases significantly [4]. Therefore, it is difficult to meet the ultra-low emission standard (<50 mg·m^{-3}) only through combustion optimization under low-load conditions. Many scholars and engineers have turned their attention to the SNCR denitrification technology, hoping to maintain a high SNCR denitrification efficiency even at low load.

It should be noted that the optimal temperature window for the SNCR reaction is 870–1050 °C (when ammonia water is used as the

* Corresponding author at: Beijing Huairou Laboratory, Beijing 100084, China.
** Corresponding author at: Tsinghua University, Beijing 100084, China.
E-mail addresses: kexiwei@sxri.hrl.ac.cn (X. Ke), lvjf@mail.tsinghua.edu.cn (J. Lyu).

https://doi.org/10.1016/j.applthermaleng.2025.127862
Received 28 June 2025; Received in revised form 2 August 2025; Accepted 11 August 2025
Available online 12 August 2025

Nomenclature

$a \sim g$	Reaction orders
$A_{(x)}$	Pre-exponential factor of each reaction
C_{NH3}	NH_3 concentration, ppm (or kmol·m^{-3})
C_{NO}	NO concentration, ppm (or kmol·m^{-3})
C_{O2}	O_2 concentration, % (or kmol·m^{-3})
d_p	Diameter of bed materials, mm (or μm)
D_t	Tube diameter, mm
$E_{(x)}$	Activation energy, kJ·mol^{-1}
h	Height, m
H_{bed}	Bed height, mm
$k_{(x)}$	Apparent reaction rate coefficient
$K_{g(m)}$	Gas mass transfer coefficient on the particle surface
m_{ash}	Mass of ash particles, g
m_{bed}	Total bed inventory, g
R_g	Molar gas constant, J·mol^{-1}·K^{-1}
$R_{(x)}$	Catalytic reaction rate per unit area (x refers to a specific chemical reaction), kmol·m^{-2}·s^{-1}
t	Time, s
T	Temperature, °C (or K)
u_{mb}	Minimum bubbling gas velocity, m·s^{-1}
u_{mf}	Minimum fluidization gas velocity, m·s^{-1}
U_{sg}	Superficial gas velocity, m·s^{-1}

Greek symbols

α_{bed}	Expansion rate of bed
$\delta_{(x,m)}$	Stoichiometric coefficient of gas $_{(m)}$ in reaction $_{(x)}$
ΔP_{base}	Pipeline pressure drop without bed material, Pa
ΔP_{bed}	Pressure drop of bed, Pa
ΔP_{total}	Total Pipeline pressure drop with bed material, Pa
ε_{bed}	Porosity of the bed layer
$\theta_{NH3/NO}$	Molar ratio of ammonia to NO
$\rho_{ash,bed}$	Density of the ash in the bed layer, kg·m^{-3}
ρ_p	Density of particles, kg·m^{-3}

Subscripts

0	Initial
NH_3-NO	Direct reduction of NO by NH_3 under anoxic conditions
NH_3-NO-O_2	Reduction of NO by NH_3 under aerobic conditions
NH_3-NO-O_2,g	Homogeneous SNCR reaction
NH_3-O_2	Oxidation of NH_3 by O_2

Abbreviations

CFB	Circulating fluidized bed
PFR	Plug-flow reactor
SNCR	Selective non-catalytic reduction
TGA	Thermogravimetric analyzers
XRD	X-ray diffraction
XRF	X-ray fluorescence spectroscopy

reducing agent) or 920–1100 °C (when urea is used as the reducing agent) [5–7]. However, under low-load conditions, the furnace temperature is relatively low. For example, the furnace outlet temperature is usually lower than 700 °C when load ratio is 30 %, which seriously deviates from the optimal temperature window of the SNCR reaction, resulting in a significant reduction in the denitrification efficiency. To address this problem, some scholars have proposed spraying appropriate denitrification synergists (such as 0.5FNW-H, Na_2CO_3, etc.) into the furnace to improve the SNCR denitrification effect. It can limitedly increase the denitrification efficiency in the temperature range of 700–850 °C but has little effect at lower temperatures [8,9].

Another technical route is to consider injecting the denitrification agent from the middle-lower part of the furnace, taking advantage of the higher temperature there to enhance the SNCR reactivity. This idea is theoretically feasible and has achieved certain results in a 350 MW supercritical CFB boiler [10]. However, it should be noted that the oxygen content in this region is also relatively high. Under specific conditions, the denitrification agent (such as NH_3) may be oxidized to generate NO_x, and injecting ammonia into the furnace may instead increase the NO_x emission [11]. Therefore, further exploration of the reaction mechanism and applicable conditions of ammonia injection in the furnace is still needed.

The above discussions mainly focus on the homogeneous reaction system. For CFB boilers, another factor that cannot be ignored is the potential catalytic and non-catalytic effect of a large number of bed materials (including ash and limestone desulfurizer) in the furnace on the conversion of nitrogen oxides. Li [12] and Wang [13] have both experimentally found that coal ash has a significant catalytic effect on the reduction of NO by CO, which is beneficial for reducing NO_x emissions. However, studies by Fu et al. [14,15]. have shown that Fe_2O_3 and CaO particles inhibit the SNCR denitrification process, narrowing the denitrification temperature window and shifting it to a higher temperature range.

Nevertheless, the actual experience of many CFB boilers shows that their denitrification efficiency can reach 60–70 %, and even 85 % under some operating conditions, exceeding the homogeneous SNCR efficiency under the same temperature conditions [16]. This may still be related to the intervention of solid particles. Therefore, the actual ammonia-based denitrification process in a CFB boiler is a hybrid process of SNCR and SCR without an additional catalyst. Currently, there are few studies on the influence of circulating ash on the NH_3+NO(+O_2) reaction system [17], and some of the research conclusions are contradictory. Fully understanding the influence of ash on the SNCR reaction under different conditions and obtaining the corresponding kinetic parameters are of great significance for optimizing ammonia-based SNCR denitrification process and reducing the NO_x emission under low-load conditions.

Commonly used devices for studying gas–solid reaction kinetics include thermogravimetric analyzers (TGA), fixed-bed reactors, and fluidized-bed reactors. One of the key aspects of relevant research is to control the external mass transfer. Usually, efforts are made to avoid or weaken the mass transfer resistance as much as possible so that the obtained apparent kinetic parameters are closer to the intrinsic kinetic parameters. Although TGA can simultaneously measure mass changes, the samples are in a stacked state, and the gas does not pass through the bed layer, resulting in a large gas external diffusion resistance [18]. For fixed-bed reactors, although there is a mature integral reactor model that can describe the axial gas flow, in many cases, the particle distribution in the bed is not uniform, and radial gas concentration gradient also exits. Meanwhile, the heat transfer performance in a fixed-bed is poor, and the endothermic or exothermic reaction itself may affect the local temperature and thus the reaction results [19].

Compared with fixed-bed reactors, bubbling-bed reactors have excellent heat and mass transfer performance. Further research shows that the smaller the tube diameter, the smaller the gas back-mixing degree, and the better the gas–solid uniformity in the reaction zone [20]. Therefore, in recent years, some scholars have proposed a micro fluidized bed reactor (usually with a tube diameter designed between 5–80 mm) [21] and the corresponding experimental method. By comparing it with traditional TGA and fixed-bed reactors, a higher apparent reaction rate has been observed [22–24].

However, few studies have focused on the gas–solid fluidization state in the micro fluidized bed and its impact on the mass transfer behavior. In practice, the fluidization velocity is usually simply set to several times the minimum fluidization velocity (u_{mf}) [25–29] to keep stable bubbling

fluidization state. Although bubbles can vigorously agitate the bed, enhancing heat and mass transfer, large bubbles may directly pass through the bed layer without fully contacting the particles (forming a gas short-circuit), resulting in incomplete reactions and reducing the overall gas conversion rate. Therefore, the overall mass transfer characteristics in the bubbling fluidization state are complex and difficult to quantitatively describe. It is necessary to pay special attention to how to select appropriate operating parameters (including particle size, gas velocity, etc.) to precisely control the fluidization state and minimize the gas mass transfer resistance in the bed.

In this paper, based on a micro fluidized bed reactor, the influence of the fluidization state on the heterogeneous reaction kinetics is explored. On this basis, three different types of circulating ash (WH anthracite coal ash, SZ bituminous coal ash, and IN lignite coal ash) were selected as samples to quantitatively analyze their catalytic effects on the SNCR reaction system, and the influence of operating parameters such as temperature, oxygen content, and initial NO concentration were discussed. The corresponding kinetic models were established, and kinetic parameters within a wide range of operating conditions were obtained. Combining with engineering practice, differentiated optimization strategies for low-load SNCR denitrification of CFB boilers were proposed.

2. Experimental section

2.1. Sample preparation

In this experiment, the ash samples were derived from three typical types of coal: Weihe anthracite coal (the designed fuel for a 660 MW ultra-supercritical CFB boiler), Shuozhou bituminous coal (the fuel used in a 350 MW supercritical CFB boiler), and Indonesian lignite coal (the fuel used in a 550 MW ultra-supercritical CFB boiler). Before the experiment, the raw coal was crushed to 0–2 mm and then placed in a muffle furnace to be fully combusted at 850 °C for 10 h. The residual ash was collected for later use.

As mentioned in the introduction, for larger and heavier Geldart's group B and group D particles, for bubbling fluidization, a considerable portion of the gas passes through the bed layer via bubbles, reducing the chance of contact with most of the particles, and resulting in uneven distribution of particles and gases. For smaller and lighter Group A particles, within a certain operating range where the gas velocity just exceeds the incipient fluidization velocity, the excess gas still enters the particle gap, causing the bed layer to expand uniformly. The particles maintain a uniform distribution in the fluid, that is, they are in a "particulate fluidization" state, ensuring uniform heat and mass transfer behavior throughout the bed and a uniform fluid residence time. Therefore, in order to control the bed material particles (including reactive ash) to be in a uniform fluidization state, achieve the maximum gas–solid contact efficiency, and minimize the interference of the overall bed mass transfer resistance on the determination of the intrinsic heterogeneous reaction kinetic parameters, the ash particles in this study were sieved, and Group A particles within the range of 88–105 μm (with a Sauter mean diameter of 95.1 μm) were selected as experimental samples.

The results of X-ray fluorescence spectroscopy (XRF) and X-ray diffraction (XRD) analyses of the three coal ash samples are shown in Fig. 1 and Fig. 2, respectively. In addition to the two common elements, Si and Al, the three coal ashes all contain different concentrations of Fe elements, and most of them exist in the form of hematite (Fe_2O_3). Among them, the iron content in IN ash is the highest, exceeding 45 %, even surpassing the contents of Si and Al. The iron content in WH ash ranks second, while the iron content in SZ ash is the lowest, less than 6 %. Many studies have pointed out that iron and its oxides have a significant catalytic or inhibitory effect on the NH_3+NO(+O_2) reaction system [30–32], which implies that the effects of the three coal ashes on the SNCR reaction may vary significantly.

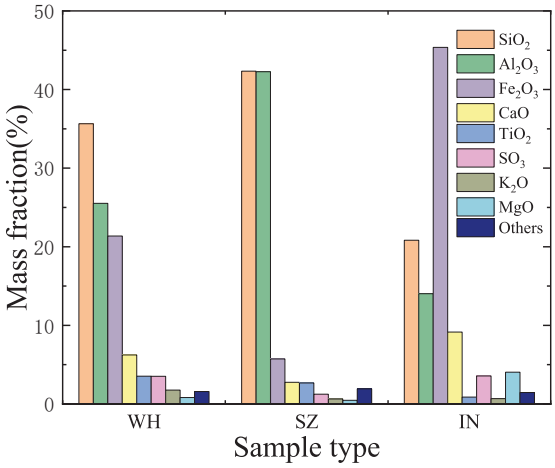

Fig. 1. Major elemental components of three typical coal ash samples (in the form of oxides).

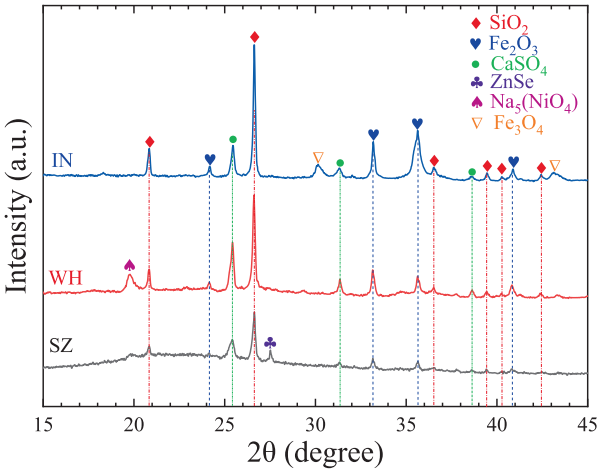

Fig. 2. XRD patterns of three typical coal ash samples.

2.2. Experimental system

The micro fluidized bed reaction system used in this study is shown in Fig. 3. This system mainly consists of a gas supply module, a reaction module, and a measurement module.

The core of the reaction module is a U-shaped reactor made of quartz glass with a height of 750 mm. It is placed inside a high-temperature resistance furnace. The height of the heating section is 430 mm, and the height of the central constant-temperature zone is approximately 200 mm. In the center of the reactor, there is a sintered quartz plate (as air distributor) with thickness of 2 mm, which is used to support solid particles and ensure the uniform passage of gas. Taking the air distributor as the boundary, the first half of the reactor consists of an inner tube (4 mm in inner diameter) and an outer tube (11 mm in inner diameter), through which gases with different properties are introduced respectively. The particle bed above the air distributor is located within the constant-temperature zone, and the inner diameter of the tube is 11 mm. The ratio of the tube diameter to the particle diameter (D_t/d_p) is approximately 116 (<150). Xu et al. have demonstrated that the gas back-mixing in the micro fluidized bed can be ignored at this value, and it is close to the plug-flow state [21].

The reactor is equipped with two groups of gas inlets. The inert gas (Ar) and the reducing gas (NH_3) are mixed and enter the reactor through the inner tube, while the mixed gas of the oxidizing gases (O_2 and NO) enter through the outer tube. The two gas streams are pre-heated and

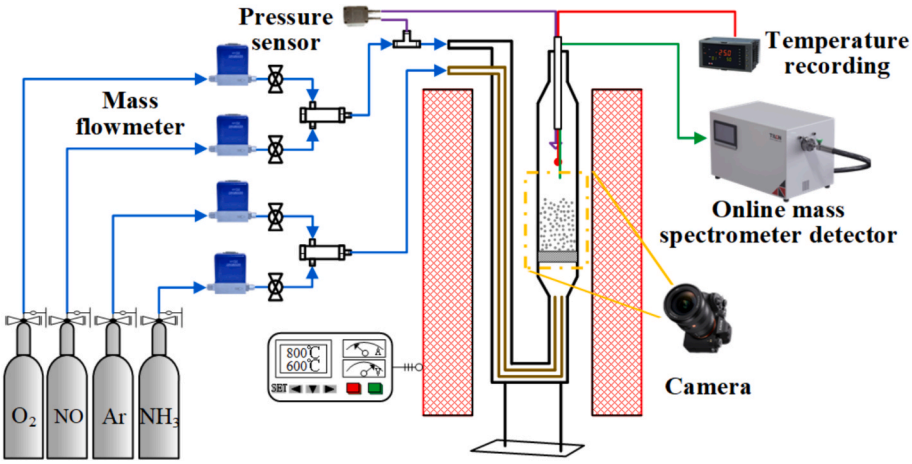

Fig. 3. Experimental system of the micro fluidized bed reactor.

only mix at a certain distance (5 mm) below the air distributor to minimize the influence of homogeneous reactions before the gas enters the fluidized bed layer. The outlet of the inner tube is designed with small holes on both sides for radial injection, making the flow directions of the two gas streams perpendicular to each other to promote uniform gas mixing.

A 0.5 mm K-type armored thermocouple is arranged on the surface of the bed layer to record the real-time temperature during experiments. The inlet of the outer tube and the outlet of the reactor are respectively connected to a pressure sensor (produced by Vadias Company in China, model RD3051-VD, with a measurement accuracy of 1 Pa) to measure the pressure drop. It should be noted that measuring the bed pressure drop needs to eliminate the influence of flow resistance in the pipeline and the reactor itself: without adding bed material, the pressure drop at the inlet and outlet of the reactor measured under U_{sg} is recorded as ΔP_{base}, and after adding bed material, the pressure drop at the inlet and outlet of the reactor measured under the same U_{sg} is recorded as ΔP_{total}, and the drop between the two is recorded as ΔP_{bed}, which is the bed pressure drop. By combining with the real-time images of the fluidized bed taken by a camera, the current gas–solid fluidization state can be determined. The outlet of the reactor is connected to an online mass spectrometer (produced by TILON Company in the UK, model LCD/SRD), which can measure the changes in the concentrations of gases such as NH_3, NO, and O_2 in real-time.

2.3. Experimental procedure and conditions

Before each experiment, a certain amount of solid particle samples are placed on the air distributor to form a static bed layer with a height of approximately 3 cm (the mass of the bed material is about 3.5 g). Under inert atmosphere (Ar), the temperature of the fluidization (reaction) region was heated from room temperature to the preset temperature. Then, the reaction gases (NO, NH_3, O_2) are introduced into the reactor. The bed material is fluidized at a specific gas speed while the gas–solid reaction occurs. When the composition of the outlet gas becomes stable, the average gas concentration within 5 min is recorded as the experimental result.

For experiments of the same type, the concentration of NO is usually below 2000 ppm [31]. It should be noted that due to the measurement uncertainty of the online mass spectrometer in this experimental system (for example, the measurement uncertainty of NO is about 20 ppm), it is difficult to conduct experiments with low NO concentrations. Otherwise, at high conversion rates, the NO concentration at the reactor outlet may be too low, resulting in inaccurate measurement results. Therefore, in this paper, the inlet NO concentration is set in the range of 1000–8000 ppm (which partially coincides with the common concentration range), and the corresponding initial ammonia-to-NO molar ratio is 0.7–1.5. Although this value is higher than the NO concentration level in the furnace under the normal combustion conditions of a CFB boiler, it has little impact on the analysis of the heterogeneous reaction mechanism and the acquisition of the corresponding kinetic parameters.

In addition, the catalytic efficiency of ash samples for the NH_3+NO (+O_2) reactions may be very high under some conditions. If the bed is formed by pure ash particles, the gas conversion rate may be close to 100 % within a wide range of conditions, making it difficult to analyze the influence of operating parameters on the reaction performance. Therefore, in this paper, a certain number of ash samples are mixed with inert quartz sand with similar physical properties for dilution, thus controlling the NO conversion rate within a reasonable range. The particle size of the quartz sand is the same as that of the ash samples to avoid obvious stratification of the two types of particles.

Before the formal kinetic experiment, first, based on the NH_3+NO reaction system (anoxic), with WH ash as the reactive bed material, at different temperatures, the fluidization gas velocity is gradually increased from zero, so as to find the point that maximizes the overall mass transfer efficiency in the bed (that is, the point with the maximum calculated apparent reaction rate), thereby determining the operational range of particulate fluidization. Each case is experimentally repeated at least 3 times to ensure the reliability of the results. The experimental operating conditions for the gas–solid fluidization classification are listed in Table 1.

Under specific gas velocity conditions (in the particulate fluidization state), the gases are changed to study the catalytic effects of coal ash on the reduction of NO by NH_3 under aerobic and anoxic conditions, respectively. For each type of coal ash sample, a total of 45 cases for the NH_3+NO reaction (anoxic) and 210 cases for the NH_3+NO + O_2 reactions (aerobic) are designed to obtain the relevant reaction kinetic

Table 1
Experimental conditions for gas–solid flow state.

Item	Unit	Value
Ash sample	/	WH coal ash
Bed temperature	T_{bed}, °C	600, 650, 700, 750, 800
Fluidization velocity	U_{sg}, mm/s	0 ~ 50
Initial NO concentration	$C_{NO,\,0}$, ppm	8000
Initial molar ratio of ammonia to NO	$\theta_{NH3/NO,\,0}$	1.0
Total bed inventory	m_{bed}, g	3.5
Mass of ash particles	m_{ash}, g	0.02
Initial bed height	$H_{bed,0}$, mm	30
Sauter mean diameter of bed materials	d_p, μm	95.1

Table 2
Experimental conditions for gas–solid reaction kinetics.

Item	Unit	Value
Bed temperature	T_{bed}, °C	600, 650, 700, 750, 800
Fluidization velocity	U_{sg}, mm/s	a specific value (related to temperature)
Initial NO concentration	C_{NO}, ppm	1000, 3000, 5000
Initial molar ratio of ammonia to NO	$\theta_{NH3/NO,\ 0}$	0.7, 0.85, 1, 1.2, 1.5
Initial O_2 concentration	$C_{O2,\ 0}$, %	0, 0.5, 1, 3, 5
Total bed inventory	m_{bed}, g	3.5
Mass of ash particles	m_{ash}, g	0.02 (WH), 0.17 (SZ), 0.02 (IN)
Initial bed height	$H_{bed,0}$, mm	30
Sauter mean diameter of bed materials	d_p, μm	95.1

parameters, as shown in Table 2. In this experiment, the temperature range is set from 600 to 800 °C, corresponding to the furnace temperature under low-load conditions for a CFB boiler.

2.4. Reaction model

For the direct reduction of NO by NH_3 catalyzed by coal ash under anoxic conditions, the overall reaction equation and the reaction rate expression are as follows:

$$4NH3 + 6NO \xrightarrow{Ash} 5N2 + 6H2O \quad \text{(R-1)}$$

$$R_{NH3\text{-}NO} = -k_{NH3\text{-}NO,\ a} C_{NH3}^{a} C_{NO}^{b} \quad (1)$$

where $R_{(x)}$ is the catalytic reaction rate per unit area (the subscript x refers to a specific chemical reaction), kmol·m^{-2}·s^{-1}; $k_{(x),a}$ is the apparent reaction rate coefficient; $C_{(m)}$ is the molar concentration of the gas (the subscript m refers to each gas component), kmol·m^{-3}.

For the NH_3+NO + O_2 reaction, it is necessary to consider the catalytic effects of coal ash on both the NO reduction and the NH_3 oxidation to generate NO, as shown in equations (R-2) and (R-3). These two reactions compete with each other. Therefore, under the catalysis of coal ash, the NO concentration at the reactor outlet may decrease (dominated by the reduction of NO by NH_3) or increase (dominated by the oxidation of NH_3 to generate NO), which means that coal ash has both positive and negative effects on the SNCR denitrification efficiency, depending specifically on reaction conditions such as temperature and gas concentration.

$$4NH3 + 4NO + O2 \xrightarrow{Ash} 4N2 + 6H2O \quad \text{(R-2)}$$

$$4NH3 + 5O2 \xrightarrow{Ash} 4NO + 6H2O \quad \text{(R-3)}$$

The reaction rate expressions for the two reactions are:

$$R_{NH_3\text{-}NO\text{-}O_2} = -k_{NH_3\text{-}NO\text{-}O_2,\ a} C_{NH_3}^{c} C_{NO}^{d} C_{O_2}^{e} \quad (2)$$

$$R_{NH3\text{-}O_2} = -k_{NH3\text{-}O2,\ a} C_{NH3}^{f} C_{O2}^{g} \quad (3)$$

As mentioned in the introduction, the heterogeneous reaction rate is also restricted by the external gas mass transfer resistance in the fluidized bed. Especially for a bubbling fluidized bed, in which catalytic efficiency is evidently affected by the bubble short-circuiting. Assuming that the catalytic effect of ash on each reaction only occurs on the particle surface, that is, gas diffusion inside the particles is not considered, the apparent reaction rate coefficient can be expressed as:

$$\frac{1}{k_{(x),\ a}} = \frac{1}{k_{(x),\ int}} + \frac{1}{K_{g(m)}} \quad (4)$$

where $K_{g(m)}$ is the gas mass transfer coefficient on the particle surface. The larger K_g is, the higher the gas mass transfer efficiency in the bed, and the closer the apparent reaction rate is to the intrinsic reaction rate; $k_{(x),int}$ is the intrinsic heterogeneous reaction rate coefficient, which is expressed in the Arrhenius form as:

$$k_{(x),\ int} = A_{(x)} \exp\left[-\frac{E_{(x)}}{RT}\right] \quad (5)$$

where $A_{(x)}$ is the pre-exponential factor of each reaction; $E_{(x)}$ is the activation energy, kJ·mol^{-1}; R is the molar gas constant, J·mol^{-1}·K^{-1}; T is the reaction temperature, K.

For the micro fluidized bed reactor in this paper, it is also necessary to establish a reactor model to obtain the kinetic parameters of each reaction based on the experimental results. Following assumptions are made:

① Since the experiment is carried out in a constant-temperature furnace, it can be approximately considered that the temperature distribution in the entire fluidized bed is uniform and remains unchanged;

② For a small-diameter tube, the radial gas concentration gradient is ignored, and only the axial concentration change is considered, that is, it is regarded as a plug-flow process;

③ Considering that the gas back-mixing in the micro fluidized bed is very weak under specific conditions [21], for the sake of simplifying the calculation, the gas axial diffusion is ignored;

④ The ash particles are uniformly distributed in the quartz sand bed material and do not affect each other, that is, it is regarded as a single-particle reaction process;

⑤ Since the concentrations of NO and NH_3 in the gas are very low (<1%), the change in the total number of moles of the gas after the reaction is not significant, and it can be considered that the gas velocity through the bed layer remains unchanged.

Based on the above assumptions, the concentrations of various gases (NO, O_2) in the micro fluidized bed under steady-state conditions satisfy the following component conservation equation:

$$\frac{U_{sg}}{\varepsilon_{bed}} \frac{dC_{(m)}}{dh} = \frac{\rho_{ash,bed}}{\rho_p} \frac{6}{d_p} \sum \left(\delta_{(x,\ m)} R_{(x)}\right) \quad (6)$$

where U_{sg} is the superficial gas velocity, m·s^{-1}; ρ_p is the density of the ash particles, kg·m^{-3}; d_p is the average particle diameter of the ash, m; $\delta_{(x,m)}$ is the stoichiometric coefficient of gas $_{(m)}$ in reaction $_{(x)}$; ε_{bed} is the porosity of the bed layer, $\rho_{ash,bed}$ is the density of the ash in the bed layer, kg·m^{-3}, both can be calculated by the following equations:

$$\varepsilon_{bed} = 1 - \frac{m_{bed}}{\rho_p H_{bed,0}(1 + \alpha_{bed})} \quad (7)$$

$$\rho_{ash,\ bed} = \frac{m_{ash}}{H_{bed,0}(1 + \alpha_{bed})} \quad (8)$$

where α_{bed} is the bed expansion ratio.

By combining Eqs. (1)–(3) and Eq. (6), and based on the measured gas concentrations at the inlet and outlet of the reactor, the reaction orders a–g and the apparent reaction rate coefficients $k_{(x),a}$ at different temperatures can be fitted.

2.5. Blank test

It should be noted that when the temperature is higher than a certain value, the SNCR reaction under homogeneous conditions also becomes significant, which will interfere with the quantitative measurement of the heterogeneous reaction rate. In this paper, a plug-flow reactor model is established using Chemkin Pro software, and the homogeneous reaction rates of NH_3+NO(+O_2) under different conditions are simulated using ÅA mechanism. The ÅA mechanism was constructed by scholars from Åbo Akademi University and other institutions, and it can better predict the SNCR reaction process within the CFB combustion temperature range [33]. The simulation results are shown in Fig. 4.

It shows that in the temperature range of 600 ~ 800 °C, under the

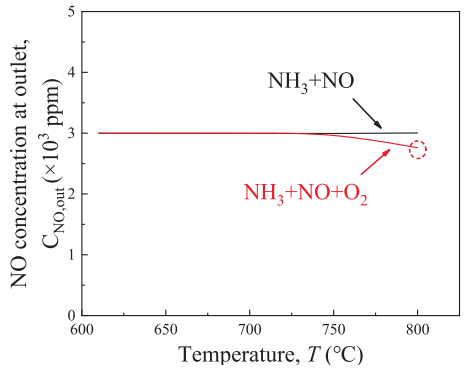

Fig. 4. NH_3 + NO (+O_2) homogeneous reaction (simulation). (PFR, t = 2 s, $C_{NO,0}$ = 3000 ppm, $C_{NH3,0}$ = 3000 ppm, $C_{O2,0}$ = 0 % or 3 %, the rest is Ar).

anaerobic condition, the reaction between NH_3 and NO hardly occurs. For the reaction of $NH_3 + NO + O_2$, it only becomes significant when the temperature is higher than 780 °C, and the reaction rate is still relatively low at 800 °C. Therefore, when the experimental data in this paper are post-processed, within the temperature condition range of 600 ~ 750 °C, the influence of the homogeneous reaction is ignored, and it is considered that the changes in the gas concentration are all the results of the heterogeneous catalytic reaction. For the working condition at 800 °C, the effect of the homogeneous reaction is taken into account when calculating the overall reaction rate of NH_3 + NO + O_2. By simulating and calculating multiple working conditions with different concentrations, the overall reaction rate at this temperature is obtained through fitting:

$$R_{NH3\text{ - }NO\text{ - }O_2,\,g}(T = 800^{\circ}C) = -8.16 \times 10^5 C_{NH3}^{1.95} C_{NO}^{0.005} C_{O2}^{0.86} \quad (9)$$

Eq. (9) is substituted into Eq. (6) for calculation, so that the catalytic reaction rate on the surface of the ash particles at 800 °C is corrected and obtained.

3. Results and discussion

3.1. Effect of gas–solid fluidization state

At room temperature, pure quartz sand particles are used as the bed material to observe the gas–solid fluidization state under different gas velocity. As shown in Fig. 5, the bed expansion ratio (α_{bed}) and the bed pressure drop (ΔP) during the process of the U_{sg} gradually increasing from zero (the rising velocity curve) and then gradually decreasing to zero (the decreasing velocity curve) are recorded.

Combining the measurement results of α_{bed} and ΔP, as well as the corresponding video image information, the gas–solid fluidization state of Group A particles at low gas velocities is roughly divided into three regions:

① Fixed bed region (green). As the U_{sg} gradually increases from zero, the ΔP approximately increases linearly, but the bed does not start to expand (α_{bed} = 1). Namely, the voids between the particles do not increase. It should be noted that the rising velocity curve and the decreasing velocity curve do not coincide in this region. During the process of the increasing U_{sg}, the bed material only starts to fluidize when the gas–solid drag force is greater than the sum of the gravity of particles and the static friction force among particles (also between particles and pipe wall); while in the fluidization state, only sliding friction exists. Since the static friction force is significantly greater than the sliding friction force, a higher ΔP is required to overcome the resistance and make the bed material fluidize during the rising velocity stage. After that, ΔP rapidly decreases to be consistent with the gravitational pressure drop of the whole particles, and the bed also starts to expand. For the decreasing velocity stage, the bed material gradually enters the static state from the fluidization state, and the changes in ΔP and α_{bed} are also more gentle. Usually, the U_{sg} corresponding to the intersection point of the rising velocity curve and the decreasing velocity curve is taken as the u_{mf}.

② Particulate fluidization region (pink). When the U_{sg} is greater than the u_{mf}, the rising velocity curve and the decreasing velocity curve basically coincide. Within a relatively narrow gas velocity range, as the U_{sg} increases, the ΔP curve basically remains unchanged, but the bed continues to expand, no obvious bubbles appear, and the bed interface is clear, indicating that the excess gas is used to increase the voids between the particles.

③ Bubbling fluidization region (orange). When the U_{sg} is greater than a certain value, the increase rate of α_{bed} significantly slows down, and the excess gas begins to pass through the bed in the form of bubbles, forming a gas short-circuit. This gas velocity is called the minimum bubbling velocity (u_{mb}). When the gas velocity is further increased, the frequency of bubble appearance is faster, the pressure signal fluctuates violently, a large number of particles are entrained out of the bed and then fall back, and the bed interface becomes blurred.

From the above analysis, it can be known that there are significant differences in the gas–solid fluidization state within different gas

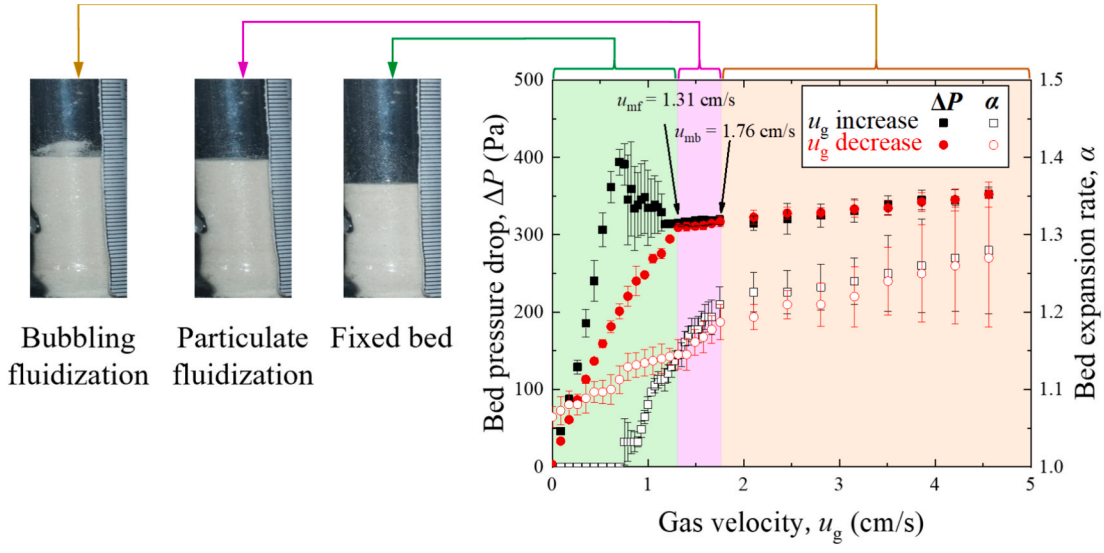

Fig. 5. Variation of the gas–solid fluidization state with the gas velocity (d_p = 95.1 μm).

velocity intervals, which affects the gas mass transfer characteristics, and then may have an obvious impact on the heterogenous reaction rate. In this paper, catalytically reactive ash particles are added to the bed to observe the changes in the gas conversion rate, as well as the calculated apparent reaction rate coefficient (k_a) under different gas velocities (fluidization states), as shown in Fig. 6. Here, the WH ash is used as the experimental sample, and the experiment is carried out for the NH_3 + NO reaction (anaerobic). The fluidization number is defined as the ratio of U_{sg} to u_{mf}.

It can be seen that at different temperatures, as the U_{sg} increases, the k_a first increases and then decreases, and the fluidization number corresponding to the maximum k_a are all between 1.0 and 1.2, namely, in the particulate fluidization operation region. As mentioned above, compared with the fixed bed, under particulate fluidization, due to the uniform fluidization of particles, the gas–solid contact is satisfied, the mass transfer resistance of external diffusion is low, and the radial concentration distribution is more uniform under the agitation of particles, which is conducive to increasing the overall reaction rate. Meanwhile, no obvious bubbles have appeared, and the gas can flow among particles more evenly. Under bubbling fluidization, due to the short-circuit effect of the bubbles, a considerable part of the gas leaves the bed in the form of bubbles without fully contacting the active particles, the overall mass transfer performance is poor, and the reaction rate decreases.

The above experimental results show that in the process of studying chemical kinetics using a micro fluidized bed reactor, it is necessary to reasonably select the operating conditions such as particle size and gas velocity (related to temperature), and precisely control the gas–solid fluidization state within the particulate fluidization region, hence minimizing the gas mass transfer resistance in the bed and make the calculated chemical kinetic parameters closer to the intrinsic values. In the following experiments, the U_{sg} is set to $1.1u_{mf}$ to ensure the particulate fluidization state, and it is considered that the calculated k_a under this condition is equal to the intrinsic heterogeneous reaction rate coefficient (k_{int}).

Referring to the experimental conditions listed in Table 2, the catalytic reaction rate coefficients of three coal ashes for the NH_3-NO reaction at different temperatures are obtained. The corresponding activation energy ($E_{NH3\text{-}NO}$) and pre-exponential factor ($A_{NH3\text{-}NO}$) are calculated according to Eq. (5), as shown in Fig. 7. The results show that under the anaerobic condition, all three coal ashes have significant catalytic effect on the reduction of NO by NH_3.

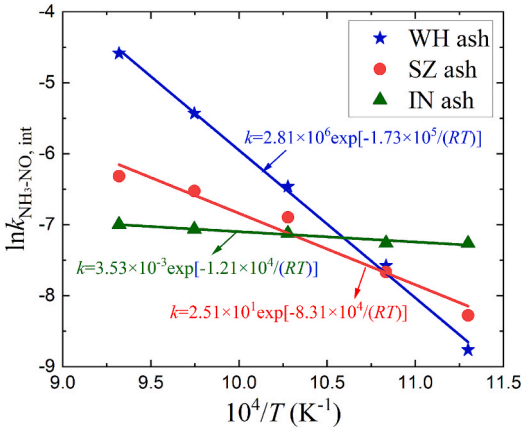

Fig. 7. Kinetic parameters of NH_3-NO reaction catalyzed by three types of coal ash under anaerobic conditions.

3.2. Catalytic effect of coal ash on NH_3 + NO + O_2 reactions

Based on the conclusions in Section 3.1, a micro fluidized bed reactor is used, and the U_{sg} is controlled at $1.1u_{mf}$ (in the particulate fluidization state). Referring to the experimental conditions listed in Table 2, the catalytic effect of coal ash on the reduction of NO by NH_3 under aerobic conditions is studied. According to the model described in Section 2.4, the catalytic reaction kinetic parameters of three kinds of coal ash for the reactions of NH_3 + NO + O_2 (R-2) and NH_3 + O_2 (R-3) are calculated, and the results are listed in Table 3. The prediction effect of this kinetic model is shown in Fig. 8. The overall calculation deviation is within ± 20 %, indicating that the two competitive reactions of (R-2) and (R-3) can well describe the catalytic effect of coal ash on the NH_3 + NO + O_2 reaction system.

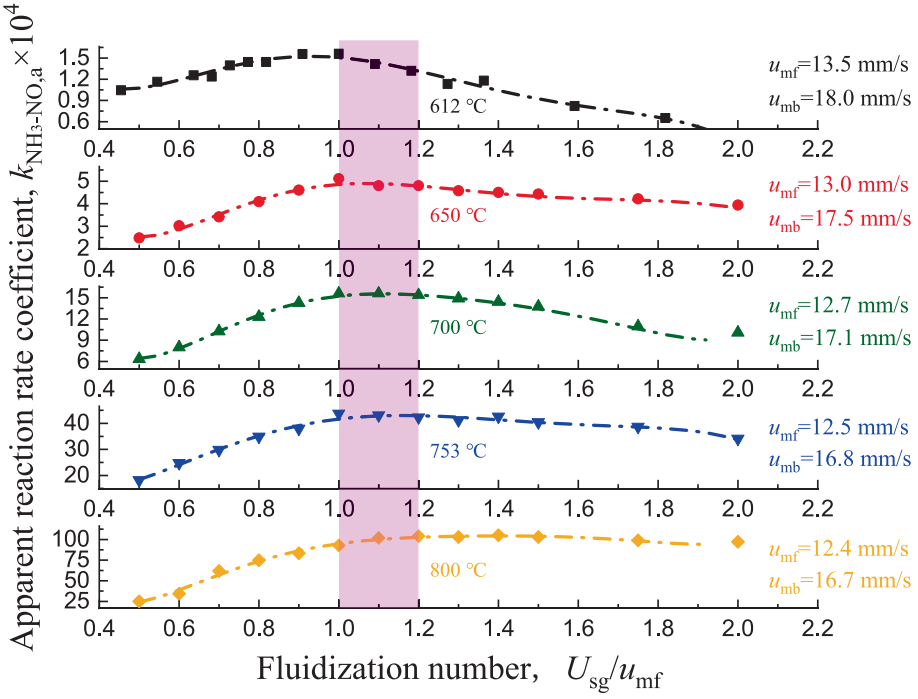

Fig. 6. Variation of the apparent reaction rate coefficient with the gas velocity at different temperatures (WH Ash, NH_3 + NO Reaction).

Table 3
Summary of the catalytic reaction kinetic parameters of three kinds of coal ash for the reaction of $NH_3 + NO + O_2$.

Reactions	$NH_3 + NO + O_2$	$NH_3 + O_2$
	$k_{NH3\text{-}NO\text{-}O2,\ int}$	$k_{NH3\text{-}O2,\ int}$
WH anthracite coal ash		
A	1.04×10^2	$8.47 \times 10^0$3674
E_a/R (K)	3026	
$c/d/e$	0.54/1.0/0.25	–
f/g	–	0.92/0.83
SZ bituminous coal ash		
A	1.87×10^1	$4.49 \times 10^1$6597
E_a/R (K)	4224	
$c/d/e$	0.51/0.77/0.61	–
f/g	–	1.0/0.72
IN lignite coal ash		
A	8.63×10^4	$3.86 \times 10^1$4059
E_a/R (K)	8460	
$c/d/e$	0.89/0.70/0.23	–
f/g	–	0.92/0.83

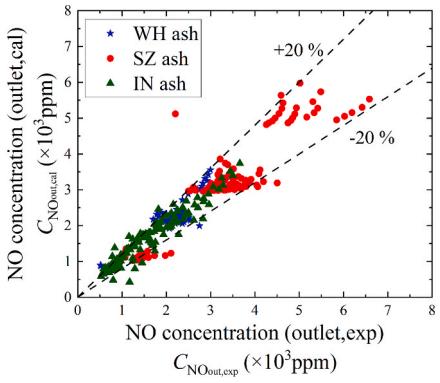

Fig. 8. Deviation of experimental and model calculation results for $NH_3 + NO + O_2$ catalytic reaction.

The experimental results show that three kinds of coal ash have catalytic effects on the NO reduction (R-2) and the NH_3 oxidation to form NO (R-3) to varying degrees, which in turn affects the actual SNCR denitrification performance under an aerobic atmosphere. Since in engineering practice, the injection amount of NH_3 usually changes with the NO emission concentration (that is, a fixed molar ratio of ammonia to NO), this paper mainly considers three factors that affect the intensity of above competitive reactions: NO concentration, O_2 concentration, and reaction temperature.

Effects of the three kinds of coal ash on the reduction of NO by ammonia are calculated in detail within the ranges of 600–900 °C for the reaction temperature, 100–1000 ppm for the NO concentration, and 0.5–21 % for the oxygen concentration (while maintaining the molar ratio of NH_3 to NO at 1.5), basically covering the atmospheric and temperature conditions at various locations in the CFB boiler furnace at wide load range. The calculation results are shown in Fig. 9.

Under the working conditions corresponding to the points located in the surface in the figure, the reaction rates of (R-2) and (R-3) are equal, namely, the two reactions reach equilibrium, and the net change rate of NO is zero, which means that the coal ash has no apparent effect on the SNCR denitrification process. In addition, the catalytic reactivity of WH ash is greatly affected by the O_2 concentration and the NO concentration, but it is relatively insensitive to the temperature. However, all three operating parameters have evident effects on the catalytic reactivity of IN ash. Since the SZ ash always shows the effect of catalyzing the oxidation of NH_3 to form NO (with an increase in the NO concentration) within this wide working condition range, the equilibrium surface for SZ ash doesn't exist.

Furthermore, by fixing the NO concentration at 300 ppm or the reaction temperature at 750 °C, respectively, the net change rate of NO under different working conditions is obtained, and a two-dimensional phase diagram is formed, as shown in Fig. 10. It can more intuitively reflect the effect of different coal ashes on SNCR denitrification (Note: The following discussion is only for the case of using ammonia as the denitrification agent).

For WH anthracite coal ash, only under the conditions of low O_2 concentration and high NO concentration (with little influence of temperature), the catalytic reduction of NO by NH_3 becomes obvious, namely, it has a positive effect on SNCR denitrification process. In engineering practice, during low-load operation, in order to ensure the safe fluidization of bed materials, excessive air is often introduced, resulting in a relatively high O_2 concentration in the middle and lower parts of the furnace. Therefore, for a CFB boiler firing WH anthracite coal, when ammonia is injected in the middle and lower parts of the furnace, although the temperature at these regions is relatively high and close to the SNCR denitrification temperature window, the coal ash may catalyze the oxidation of NH_3 to form NO, weakening the SNCR denitrification efficiency. The ideal ammonia injection position should still be at the upper part of the furnace or at the inlet of the cyclone, where the oxygen concentration is low. Or technologies such as flue gas recirculation can

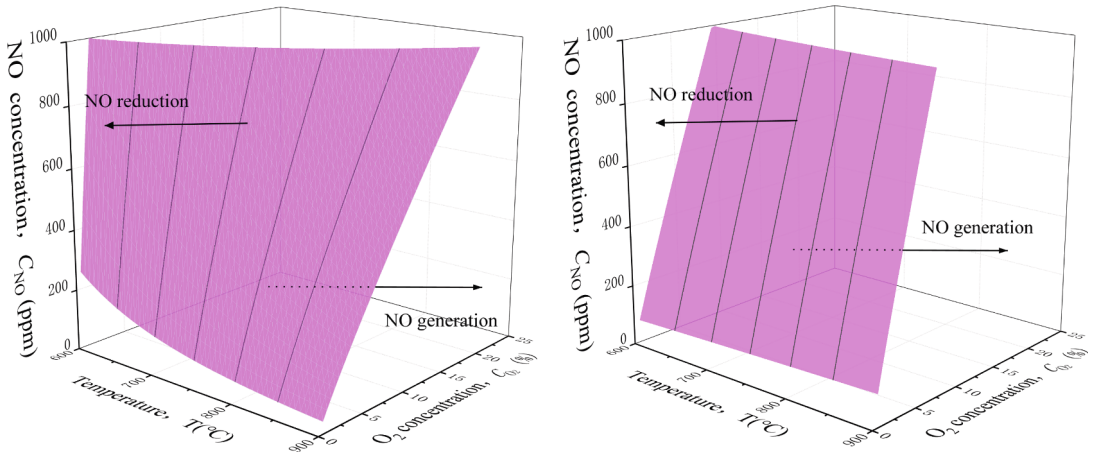

Fig. 9. Equilibrium surface of NO reduction rate and generation rate.

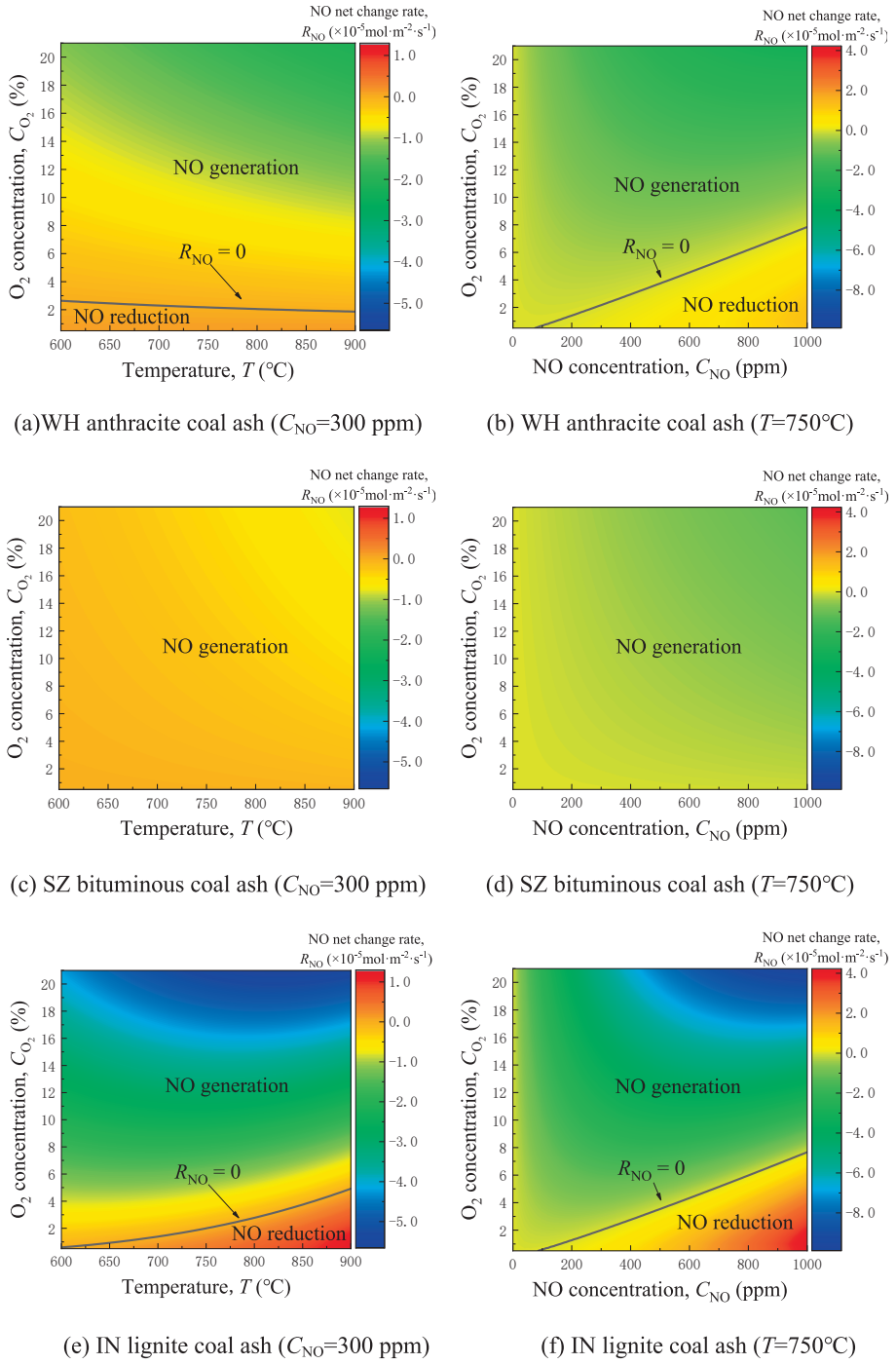

Fig. 10. Changes in net rate of change of NO under specific NO concentration and temperature conditions.

be adopted to reduce the O_2 concentration in the furnace.

For SZ bituminous coal ash, since it mainly shows the catalytic oxidation of NH_3 to form NO within a wide operating parameters range, the presence of ash always weakens the SNCR denitrification efficiency. It is advisable to consider arranging the ammonia injection port at the outlet of the cyclone, where the ash concentration is very low, thus avoiding the negative effects caused by the catalysis of the ash.

For IN lignite coal ash, generally speaking, the higher the temperature, the lower the O_2 concentration, and the higher the NO concentration, the more significant the catalytic reactivity of the ash on the reduction of NO by NH_3. Compared with WH ash, the catalytic effect of IN ash is more sensitive to temperature, and the operational region related to the NO reduction zone is slightly wider. Therefore, in engineering practice, it can be considered to arrange the ammonia injection port in the furnace and move it down appropriately, thus taking advantage of the relatively high bed temperature in the middle and lower parts of the furnace under low load, which can not only significantly increase the homogeneous SNCR reaction rate, but also make use of the catalytic effect of the coal ash on this reaction.

4. Conclusions

Facing the demand for large-scale integration of renewable energy power such as wind power and photovoltaic power, an increasing number of CFB coal-fired power generation units need to operate at low-load for a long time. The control of NO_x emissions in a wide load range,

especially under low-load conditions, has become one of the key factors restricting the deep peak regulation capacity of CFB boilers. In this paper, a micro fluidized bed reactor is used to quantitatively analyze the catalytic effect of three typical coal ashes on the NH_3 + NO(+O_2) reactions, and a relevant chemical kinetic model is established. Then, the potential influence of circulating ash particles in the furnace on the ammonia-based SNCR denitrification is deeply explored.

It is found through experiments that the gas mass transfer characteristics in the micro fluidized bed are significantly different under different gas–solid fluidization states, which in turn affects the apparent chemical reaction rate. For Group A particles, by controlling the superficial gas velocity to be 1.0 to 1.2 times the minimum fluidization velocity and keeping the stable particulate fluidization state, it can be ensured that the external gas mass transfer resistance is low, so that the calculated heterogenous reaction kinetic parameters are closer to the intrinsic values.

Based on the micro fluidized bed experimental method with fluidization state regulation and the kinetic model of dual competitive reactions, the kinetic parameters of NH_3 + NO(+O_2) catalytic reactions are obtained. It is found that under aerobic conditions, due to the simultaneous existence of the rival SNCR reaction (NO reduction) and NH_3 oxidation reaction (NO generation), the NO concentration may change in different directions. For WH anthracite coal ash and IN lignite coal ash, the catalytic reduction effect on NO is only obvious under the conditions of low oxygen and relatively high NO concentration, and the IN ash is more sensitive to temperature. However, for SZ bituminous coal ash, it mainly shows the catalytic oxidation of NH_3 to form NO under wide working conditions, which means that the presence of this ash always weakens the effect of SNCR denitrification.

The research of this paper shows that the reactive bed material has a catalytic effect on nitrogen-containing chemical reactions such as SNCR, and the catalytic effect is affected by temperature, O_2 concentration and NO concentration. In the future, by means of numerical simulation, intelligent monitoring and other methods, it is possible to accurately construct the temperature field, gas–solid flow field and atmosphere field in the CFB boiler furnace within a wide load range. Through precise ammonia injection in different zones of the furnace, the positive impact of ash catalysis on SNCR denitrification can be fully utilized, so as to minimize NO emissions.

CRediT authorship contribution statement

Ling Jiang: Writing – original draft, Methodology, Validation, Formal analysis, Visualization, Investigation, Data curation. **Xueyu Tang:** Investigation, Validation. **Dan Li:** Writing – review & editing, Validation. **Bingjun Du:** Software, Investigation. **Xin Yu:** Validation. **Zhong Huang:** Supervision. **Xiwei Ke:** Writing – review & editing, Supervision, Conceptualization, Resources, Funding acquisition, Project administration. **Junfu Lyu:** Supervision, Resources, Funding acquisition, Project administration.

Declaration of competing interest

The authors declare that they have no known competing financial interests or personal relationships that could have appeared to influence the work reported in this paper.

Acknowledgment

This research was supported by the National Natural Science Foundation of China (No. 52306251) and the Program of Beijing Huairou Laboratory (ZD2023008A).

Data availability

Data will be made available on request.

References

[1] X. Ke, S. Zhu, Z. Huang, M. Zhang, J. Lyu, H. Yang, T. Zhou, Issues in deep peak regulation for circulating fluidized bed combustion: Variation of NOx emissions with boiler load, Environ. Pollut. 318 (2023).
[2] G.X. Yue, R.X. Cai, J.F. Lu, H. Zhang, From a CFB reactor to a CFB boiler - the review of R&D progress of CFB coal combustion technology in China, Powder Technol. 316 (2017) 18–28.
[3] X.W. Ke, Y.G. Yao, Z. Huang, M. Zhang, J. Lyu, H.R. Yang, T. Zhou, Prediction and minimization of NOx emission in a circulating fluidized bed combustor: improvement of bed quality by optimizing cyclone performance and coal particle size, Fuel 328 (2022).
[4] K. Li, Y. Qu, Y. Zheng, Z. Zhang, Analysis and response measures of NOx low lord formation characteristics in 300 MW CFB and countermeasures, Northeast Electric Power Technol. 40 (2019) 46–49.
[5] H.Z. Liu, S. Zhao, C.F. You, H.M. Wang, Experimental Study of the enhancement of the selective noncatalytic reduction denitrification process with methane and propane in a circulating fluidized bed, Ind. Eng. Chem. Res. 58 (2019) 7825–7833.
[6] W.Y. Fan, T.L. Zhu, Y.F. Sun, D. Lv, Effects of gas compositions on NOx reduction by selective non-catalytic reduction with ammonia in a simulated cement precalciner atmosphere, Chemosphere 113 (2014) 182–187.
[7] W. Zhou, D. Moyeda, V. Lissianski, J.Y. Chen, Development and implementation of numerical simulation for a selective noncatalytic reduction system design, Ind. Eng. Chem. Res. 48 (2009) 10994–11001.
[8] H. Liu, Y. Zhang, H. Wang, C. You, Performance of Fe-Ni-W exchanged zeolite for NOx reduction with NH3 in a lab-scale circulating fluidized bed, Fuel 307 (2022).
[9] X. Wei, C. Luo, G. Wu, S. Ma, Experimental study on low temperature synergistic denitration of circulating fluidized bed based on low nitrogen combustion, J. Eng. Therm. Energy Power 38 (2023) 84–89.
[10] J. Yang, J. Wang, P. Wang, F. Wang, F. Yang, Characterization and mitigation of NOx emissions across a wide load range in supercritical 350 MW circulating fluidized bed boiler, Clean Coal Technol. 31 (2023) 78–85.
[11] A. Jensen, J.E. Johnsson, Modelling of NOx emissions from pressurized fluidized bed combustion - a parameter study, Chem. Eng. Sci. 52 (1997) 1715–1731.
[12] J. Li, Y. Zhang, H. Yang, Y. Yang, Study of the effect of ash composition in coal on the kinetic parameters of NO reduction reaction by CO, J. China Coal Soc. 41 (2016) 2448–2453.
[13] C.A. Wang, Y. Du, D. Che, Investigation on the NO reduction with coal char and high concentration CO during oxy-fuel combustion, Energy Fuel 26 (2012) 7367–7377.
[14] S.-L. Fu, Q. Song, J.-S. Tang, Q. Yao, Effect of CaO on the selective non-catalytic reduction deNOx process: experimental and kinetic study, Chem. Eng. J. 249 (2014) 252–259.
[15] S.-L. Fu, Q. Song, Q. Yao, Experimental and kinetic study on the influence of iron oxide on the selective noncatalytic reduction DeNOx process, Ind. Eng. Chem. Res. 53 (2014) 5801–5809.
[16] X. Ke, R. Cai, J. Lyu, M. Zhang, Y. Wu, H. Yang, H. Zhang, Research progress of the effects of Ca-based sorbents on the NOx reaction in circulating fluidized bed boilers, Clean Coal Technol. 25 (2019) 1–11.
[17] W. Fan, X. Wu, H. Guo, J. Zhu, P. Liu, C. Chen, Y. Wang, Experimental study on the impact of adding NH3 on NO production in coal combustion and the effects of char, coal ash, and additives on NH3 reducing NO under high temperature, Energy 173 (2019) 109–120.
[18] F. Hu, B. Xiong, X. Huang, Z. Liu, Theoretical analysis and experimental verification of diminishing the diffusion influence on determination of char oxidation kinetics by thermo-gravimetric analysis, Energy 275 (2023).
[19] T. Ferreira, J.M. Paiva, C. Pinho, Comparative analysis of fluidized and fixed beds to obtain data on the char pellet's combustion regime, Int. J. Energy Clean Environ. 21 (2020) 237–268.
[20] S. Geng, J. Yu, J. Zhang, H. Guo, J. Yue, G. Xu, Gas back-mixing in micro fluidized beds, J. Chem. Ind. Eng. 64 (2013) 867–876.
[21] Z.N. Han, J.R. Yue, S.L. Geng, D.D. Hu, X.J. Liu, S.B. Suleiman, Y.B. Cui, D.R. Bai, G.W. Xu, State-of-the-art hydrodynamics of gas-solid micro fluidized beds, Chem. Eng. Sci. 232 (2021).
[22] Y. Zhu, Q. Wang, K. Li, J. Cen, M. Fang, C. Ying, Study on pressurized isothermal pyrolysis characteristics of low-rank coal in a pressurized micro-fluidized bed reaction analyzer, Energy 240 (2022) 122475.
[23] R. Li, H. Liu, J. Liu, C. Wu, Y. Zou, Y. Zhang, Catalytic CO2 gasification of coal char with Ca/K compounds in a mic-fluidized bed reactor, Energy 322 (2025) 135333.
[24] J. Yu, C.B. Yao, X. Zeng, S. Geng, L. Dong, Y. Wang, S.Q. Gao, G.W. Xu, Biomass pyrolysis in a micro-fluidized bed reactor: Characterization and kinetics, Chem. Eng. J. 168 (2011) 839–847.
[25] S.J. Wu, S.H. Wang, Z.S. Li, Evaluation of biomass char combustion kinetics using a micro-fluidized bed with thermogravimetry-mass spectrometry, Energy Fuel 37 (2023).
[26] Q. Wang, C.X. Zhang, Z.X. Zhu, M.T. Arslan, L. Yang, F. Wei, Comparison study for the oxidative dehydrogenation of isopentenes to isoprene in fixed and fluidized beds, Catal. Today 276 (2016) 78–84.
[27] H. Wang, Z.S. Li, Y. Li, N.S. Cai, Reduced-order model for CaO carbonation kinetics measured using micro-fluidized bed thermogravimetric analysis, Chem. Eng. Sci. 229 (2021).
[28] Y. Li, Z.S. Li, H. Wang, N.S. Cai, CaO carbonation kinetics determined using micro-fluidized bed thermogravimetric analysis, Fuel 264 (2020).
[29] S.L. Geng, Z.N. Han, Y. Hu, Y.B. Cui, J.R. Yue, J. Yu, G.W. Xu, Methane Decomposition Kinetics over Fe2O3 Catalyst in Micro Fluidized Bed Reaction Analyzer, Ind. Eng. Chem. Res. 57 (2018) 8413–8423.

[30] S.S. Daood, T.S. Yelland, W. Nimmo, Selective non-catalytic reduction - Fe-based additive hybrid technology, Fuel 208 (2017) 353–362.
[31] M.-X. Xu, Y.-C. Wu, N. Liu, H.-D. Ouyang, Q. Lu, Experimental investigation into NO removal over circulating ash in selective noncatalytic reduction during circulating fluidized bed combustion, Ind. Eng. Chem. Res. 59 (2020) 9451–9458.
[32] C.H. Ma, H.Y. Tian, Y.C. Ma, B.J. Du, Y. Zhang, J. Lyu, X.W. Ke, Experimental investigation on the effect of iron-rich coal ash on biomass-volatile combustion characteristics in the fluidized bed, Energy 321 (2025).
[33] E.C. Zabetta, M. Hupa, A detailed kinetic mechanism including methanol and nitrogen pollutants relevant to the gas-phase combustion and pyrolysis of biomass-derived fuels, Combust. Flame 152 (2008) 14–27.